Chemical Bulletin of "Politehnica" University of Timisoara, ROMANIA
Series of Chemistry and Environmental Engineering
Chem. Bull. "POLITEHNICA" Univ. (Timisoara) ***Volume 59(73), 2, 2014***

Barium Hexaferrite Synthesis via the Citrate Method

R. Babuta, I. Lazau, C. Pacurariu and R.I. Lazau

POLITEHNICA University of Timisoara, Faculty of Industrial Chemistry and Environmental Engineering, 6 Vasile Parvan Blvd., 300223, Timisoara, Romania, e-mail: babuta.roxana@yahoo.com

Abstract: Barium ferrites, particularly M-type with hexagonal molecular structure – $BaFe_{12}O_{19}$, represent important magnetic materials with applications in: wireless communication, electronic devices, microwave absorbing agents, magnetic recording media. This paper deals with the formation of barium hexaferrite via the citrate method. Starting from $Ba(NO_3)_2$, $Fe(NO_3)_3 \cdot 9H_2O$ and citric acid monohydrate with ammonia solution addition until reaching pH=8, a precursor which self-ignites at 300 °C was obtained. After the auto-combustion reaction, a reddish brown to brown-gray powder resulted, which was annealed at different temperatures. The use of citric acid in excess and ammonia is justified in the case of barium hexaferrite formation. The results have pointed out that is possible to obtain $BaFe_{12}O_{19}$ as single phase after annealing at 800 °C/1h.

Keywords: barium hexaferrite, citric acid, pH, auto-combustion

1. Introduction

Barium hexaferrite, $BaFe_{12}O_{19}$, also known as barium M ferrite, has magnetoplumbite structure. In the past time, barium hexaferrite raised major interest both in terms of technology and science, as comprehensive studies were developed on obtaining and characterization of this material, which reaches an annual production of 300.000 tons [1].

Due to the remarkable properties [2]: high Curie temperature, excellent stability, corrosion resistance and good mechanical strength, barium hexaferrite is used in: electronics industry [3], the absorption of microwave radiation [4, 5], obtaining permanent magnets and magnetic fluids [6, 7], producing data storage devices [3, 8].

Considering that the preparation method plays a key role in determining barium hexaferrite properties, researchers have focused on the use of unconventional methods: sol-gel [9], coprecipitation [10, 11] autocombustion of polymeric precursors [12, 13], oxalate route [14], hydrothermal [15] or microemulsion [16]. These methods allow reducing the formation temperature of $BaFe_{12}O_{19}$ and a better control over the size and shape of the particles, the degree of crystallinity and magnetic properties.

A new direction in the use of magnetic powders is as adsorbents in water remediation processes [17]. In this case, the major advantage of magnetic powders is the easy separation using an external magnetic field [18]. Considering $BaFe_{12}O_{19}$ a potential adsorbent with magnetic properties, the major interest is to keep the formation temperature as low as possible, using non-conventional methods, to provide high surface area.

Citrate method seems to be the most suitable for the synthesis of $BaFe_{12}O_{19}$ powders with adsorbent properties. This method is based on iron and barium nitrate, to which was added citric acid for chelation of Fe^{3+} and Ba^{2+} cations. Heating the solution a viscous gel is formed, the method being sometimes considered sol-gel. On further heating the gel self-ignites, justifying the method name "sol-gel auto-combustion method" [12].

The literature data on $BaFe_{12}O_{19}$ synthesis by citrate method indicates the possibility of formation starting at temperatures of 800 °C, in the case of pH correction [19]. Qiu et al [20] reported the pH correction necessity in order to lower the formation temperature of $BaFe_{12}O_{19}$ from a mixture of barium nitrate, iron nitrate and glycine.

Regarding the proportion in which citric acid must be used and the intermediate phase transformations of the precursor until the compound is formed, information is far from being clear; however, previous studies confirmed the positive effect of citric acid excess, related to iron nitrate and barium nitrate [12, 21].

Accordingly, the aim of this paper is to systematically track $BaFe_{12}O_{19}$ formation from iron and barium nitrates, highlighting the need of citric acid, pH correction by ammonia addition and the effect of citric acid excess.

2. Experimental

Pro analysi barium nitrate (Merck), iron nitrate nonahydrate (Merck), citric acid (Chimopar) and ammonia solution 25% (Chimopar) were used. The composition of the investigated samples is presented in Table 1.

The molar ratio $Ba(NO_3)_2$: $Fe(NO_3)_3$: $C_6H_8O_7$ = 1: 12: 13 was considered stoichiometric, in which citric acid, tribasic, ensures Ba^{2+} and Fe^{3+} chelatization; the theoretical amount of citric acid (38/3 moles) was rounded up to 13 moles. Experimental determinations were performed in order to obtain 0.005 moles of barium hexaferrite.

Barium and iron nitrate were dissolved in the minimum necessary amount of distilled water at 80 ° C, under magnetic stirring, with the formation of an orange solution. The citric acid needed for barium and iron ions chelatization was dissolved separately. When the two

solutions were mixed into a capsule, a reddish brown solution was formed. The temperature on the hotplate was raised until the water evolved and a highly viscous brown gel was formed

In the case of pH correction, in order to create the necessary basic medium for the reaction, the calculated amount of ammonia solution was added. A color change from reddish brown solution to light green was noticed. After water removal from the system while heating on the hotplate, a highly viscous black-green gel was formed.

On further heating, the sample self-ignites at around 300 °C, becoming incandescent or engulfed with flames, depending on the characteristics of the precursor. The result is a powder colored from reddish brown to brown-gray, or even black. The obtained powders were subjected to heat treatment in the oven at various temperatures, in air atmosphere.

The obtained powders were characterized in terms of phase composition by X-ray diffraction using a Rigaku Ultima IV diffractometer, CuKα radiation. The behavior of the samples upon heating was studied by means of thermal analysis using a Netzsch STA 449C instrument, in air atmosphere, at a flow rate of 20 mL min^{-1}. TG / DSC curves were recorded in the temperature range 25-1000 °C at a heating rate of 10 K min^{-1}, using alumina crucibles. The specific surface area was determined by BET technique, N_2 adsorption-desorption, using a Micromeritics ASAP 2020 instrument.

3. Results and Discussion

Table 2 shows the phase composition of the obtained powders directly after self-ignition and after annealing at different temperatures.

Identification cards:
α-Fe_2O_3: 01-089-0596, $BaFe_{12}O_{19}$: 00-039-1433,
α- $BaFe_2O_4$: 00-027-1030, $BaCO_3$: 00-044-1487,
γ-Fe_2O_3:04-007-2140.

TABLE 1. The composition of the studied samples

Sample No.	Molar ratio				pH	Observation
	$Ba(NO_3)_2$	$Fe(NO_3)_3$	Citric acid	NH_3		
1	1	12	-	-	1	-
2	1	12	-	41.8	8 – 8.5	Brown precipitate
3	1	12	13	-	0.5 – 1	Incandescence
4	1	12	13	84.7	8	Combustion with intense flames
5	1	12	26	127.6	8	Combustion with flames
6	1	12	52	213.4	8	Prolonged incandescence

TABLE 2. Phase composition of the studied samples

Sample No.	Phase composition				
	After auto-combustion	650 °C/ 3h	800 °C/ 1h	900 °C/ 1h	1000 °C/ 1h
1	-	-	α-Fe_2O_3 $BaFe_{12}O_{19}$ α-$BaFe_2O_4$	-	α-Fe_2O_3 $BaFe_{12}O_{19}$ α-$BaFe_2O_4$
2	-	-	$BaFe_{12}O_{19}$ α-$BaFe_2O_4$ α-Fe_2O_3	-	$BaFe_{12}O_{19}$ α- $BaFe_2O_4$ α-Fe_2O_3
3	-	-	α-Fe_2O_3 α- $BaFe_2O_4$ $BaFe_{12}O_{19}$	-	α-Fe_2O_3 $BaFe_{12}O_{19}$ α- $BaFe_2O_4$
4	γ-Fe_2O_3 α-$BaFe_2O_4$ α-Fe_2O_3 $BaCO_3$	γ-Fe_2O_3 α-$BaFe_2O_4$ $BaFe_{12}O_{19}$	$BaFe_{12}O_{19}$ α-Fe_2O_3 (traces) S_{BET}= 5,6 m^2/g	$BaFe_{12}O_{19}$	$BaFe_{12}O_{19}$ S_{BET}= 3,2 m^2/g
5	γ-Fe_2O_3 α-$BaFe_2O_4$ α-Fe_2O_3	γ-Fe_2O_3 α-$BaFe_2O_4$ α-Fe_2O_3 $BaFe_{12}O_{19}$	$BaFe_{12}O_{19}$	-	$BaFe_{12}O_{19}$
6	γ-Fe_2O_3 $BaCO_3$	$BaFe_{12}O_{19}$ α-$BaFe_2O_4$ γ-Fe_2O_3 α-Fe_2O_3	$BaFe_{12}O_{19}$	-	$BaFe_{12}O_{19}$

Figure 1 presents the X-ray diffraction patterns of samples 1 and 2, annealed at 1000 °C for 1 hour. It is noted that beside the projected phase – $BaFe_{12}O_{19}$, even after calcination at 1000 °C, two more phases are present: α-Fe_2O_3 and α-$BaFe_2O_4$. $BaFe_{12}O_{19}$ proportion in the powder calcined at 1000 °C is significantly higher in sample 2 than sample 1.

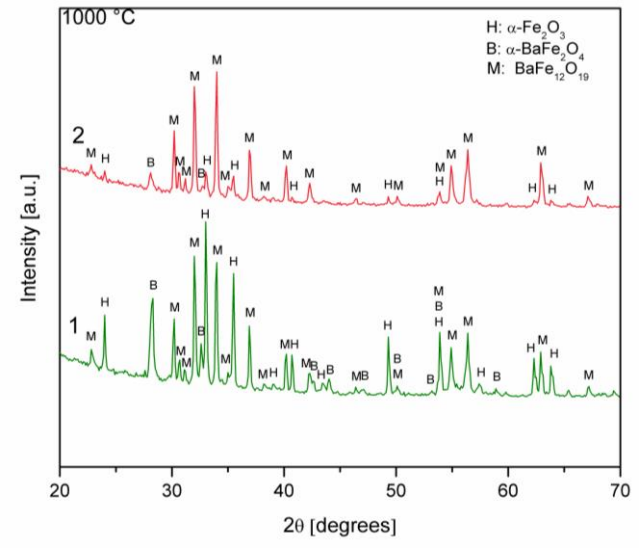

Figure 1. XRD patterns of samples 1 and 2, annealed at 1000 °C/ 1h.

Figures 2 and 3 show the thermal behaviour of samples 1 and 2 precursors.

For sample 1 (Fig. 2), DSC and TG curves for temperatures up to 250 °C correspond to the thermal behavior of $Fe(NO_3)_3 \cdot 9H_2O$ [22]. The endotherm effect with maximum at 575.2 °C, accompanied by mass loss can be assigned to the decomposition of the fine dispersed $Ba(NO_3)_2$, mixed with Fe_2O_3 formed by the decomposition of the ferric nitrate.

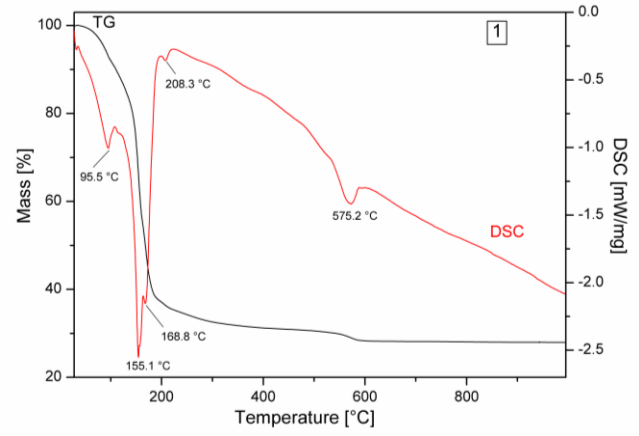

Figure 2. TG and DSC curves of the sample 1 precursor

The reaction between BaO and Fe_2O_3, with formation of $BaFe_2O_4$ and $BaFe_{12}O_{19}$ occurs gradually at temperatures around 800 °C. Increasing the temperature to 1000 °C does not ensure the formation of hexaferrite; α-Fe_2O_3 remains the main phase.

In the case of sample 2, $Fe_2O_3 \cdot xH_2O$ and $Ba(OH)_2$ coprecipitate mixed with NH_4NO_3, formed during the addition of NH_3 solution, the thermal behavior is shown in Figure 3. The endothermic effects below 200 °C are assigned to water removal and $Fe_2O_3 \cdot xH_2O$ decomposition, with Fe_2O_3 formation. The exothermic effect at 279.6 ° C is assigned to NH_4NO_3 highly exothermic decomposition. The weak endothermic effect at 557.9 ° C is due to $Ba(OH)_2$ decomposition.

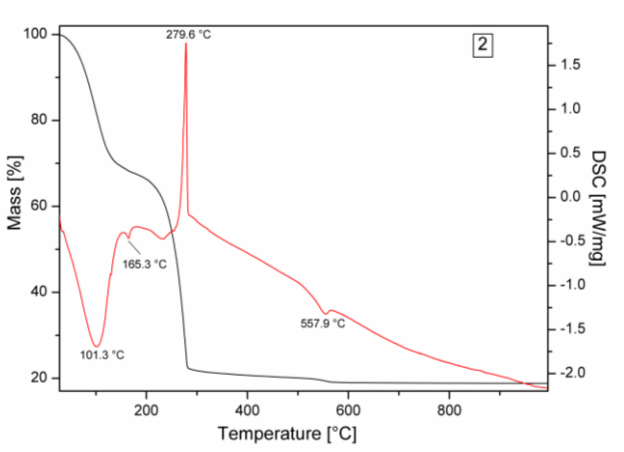

Figure 3. TG and DSC curves of the sample 2 precursor

The proportion of $BaFe_{12}O_{19}$ formed at 800 °C and 1000 °C, is higher in the case of sample 1 than sample 2, which is also confirmed by the X-ray diffraction patterns (Figure 1). This reflects a higher reactivity of the mixture obtained by co-precipitation. However, this reactivity is not high enough to ensure the designed compound formation as single phase, at temperatures below 1000 °C.

Samples 3, 4, 5 and 6 were obtained from iron and barium nitrate treated with citric acid; in samples 3 and 4, the amount of citric acid is stoichiometric: without pH correction in the sample 3 and with pH correction (8÷8.5) by NH_3 solution addition in the sample 4. Samples 5 and 6 differ from the sample 4 by the use of citric acid in excess, and thus a higher proportion of NH_3.

The X-ray diffraction patterns of samples 3, 4 and 5 after annealing at 800 °C for 1 hour, are presented in Fig.4. It is noted that in the sample 3 (without pH adjustment) the main phase is hematite at 800 °C, while the hexaferrite is present only in a small proportion. This demonstrates that the use of citric acid as chelating agent for Ba^{2+} and Fe^{3+} is not sufficient to ensure the formation of the projected phase at 800 °C.

pH correction (at value 8) by NH_3 solution addition (sample 4) essentially changes the situation: hexaferrite is the main phase, alongside traces of hematite. The situation is even better in the case of sample 5, with an excess of citric acid (twice the stoichiometric amount) and thereby the corresponding ammonia addition. So, in this sample, after calcination at 800 °C, $BaFe_{12}O_{19}$ is present as single phase.

$BaFe_{12}O_{19}$ powder calcined at 800 °C has a relatively high surface area of 5.6 m^2/g. By raising the calcination temperature at 1000 °C, the specific surface area decreases

to 3.2 m^2/g. This indicates that in the case of using barium hexaferrite powder as adsorbent in water depollution, it is essential that the calcination temperature does not exceed 800 °C.

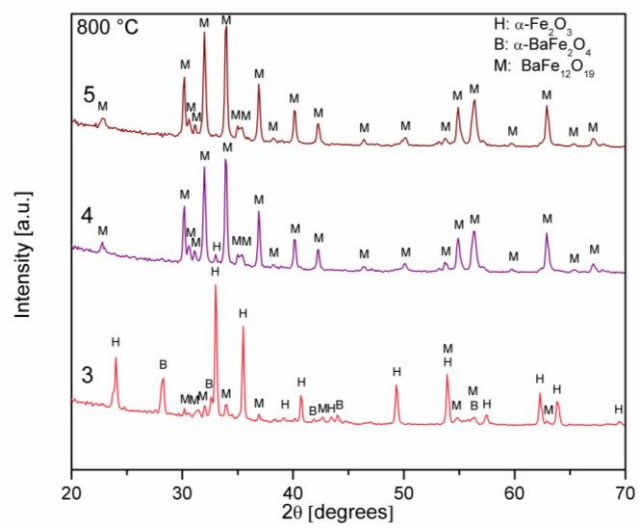

Figure 4. XRD patterns for samples 3, 4 and 5, annealed at 800 °C/ 1h

Sample 6 presents an even slightly better behavior, when the citric acid excess is greater (4 times the amount required). A better behavior compared to sample 5, is also reflected in the higher proportion of $BaFe_{12}O_{19}$, in the sample calcined at 650 °C. Fig. 5 presents the XRD patterns of sample 6 calcined at different temperatures; $BaFe_{12}O_{19}$ is the single phase at 800 °C and by raising the temperature to 1000 °C, the intensity of the diffraction peaks increases, showing larger crystallite size.

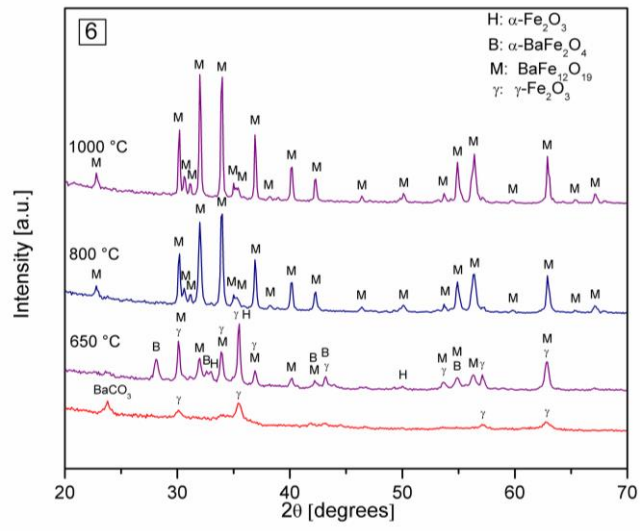

Figure 5. XRD patterns for samples 6, annealed at different temperatures.

Thermal behavior of samples 5 and 6, pursued by thermal analysis is shown in Fig. 6 and Fig. 7.

Viscous gel samples were picked for the analysis, formed after mixtures heating. An endothermic effect is observed around 200 °C, in both cases; that is attributed to the start of citrate component decomposition, followed by a sequence of exothermic processes due to oxidative degradation of the decomposition products. These processes also involve the exothermic decomposition of ammonium nitrate present in the mixtures.

Heated on a hotplate in a capsule the sample ignites, due to the exothermic processes, followed by the auto-combustion, with γ-Fe_2O_3 powder formation. Ba^{2+} cations are most likely in the form of $BaCO_3$ intimately distributed in a mixture with γ-Fe_2O_3. $BaCO_3$ decomposition does not show any effect, on TG curves, which can be explained by the important mass difference between the sample in the capsule and the sample taken for analysis.

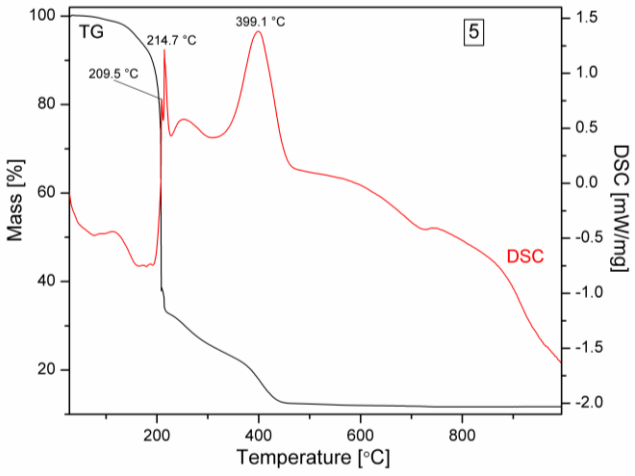

Figure 6. TG and DSC curves of the sample 5 precursor

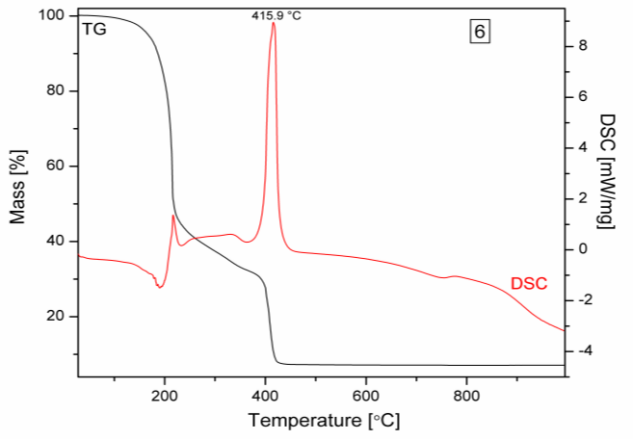

Figure 7. TG and DSC curves of the sample 6 precursor

The results prove that in the case of $BaFe_{12}O_{19}$ formation, the chelatization process of Fe^{3+} and Ba^{2+} cations, specific to citrate method (sample 3), practically does not bring any improvement compared to the nitrates mixture (sample 1). But co-precipitation, by NH_3 addition (Sample 2) has an obvious positive effect compared to samples 1 and 3.

Things change essentially when the chelatization of Fe^{3+} and Ba^{2+} cations using citric acid takes place first and is followed by pH correction. The positive effect in this case may be assigned to the presence in the precursor

mixture of both ammonium nitrate and ammonium citrate, with a very homogeneous distribution of Fe^{3+} and Ba^{2+} cations. During NH_3 decomposition and thermal degradation of citrate component in a relatively wide temperature range, γ-Fe_2O_3 results intimately associated with $BaCO_3$, which ensures a significant increase in the mixtures reactivity; $BaFe_{12}O_{19}$ is practically single-phase at 800 °C. This thermal behavior of the samples, is upholded by the positive effect of citric acid excess and thus, NH_3 presence (twice the stoichiometric amount required or even more).

4. Conclusions

The results show that it is possible to obtain $BaFe_{12}O_{19}$ at 800 °C, using citrate method, in which the pH correction (to value 8) by ammonia addition proved to be very important.

$BaFe_{12}O_{19}$ powder calcined at 800 °C has a relatively high surface area of 5.6 m^2/g; by raising the temperature at 1000 °C the specific surface area decreases to 3.2 m^2/g.

The positive effect in using citric acid and ammonia in excess, on $BaFe_{12}O_{19}$ formation was confirmed. It is justified an excess of two times, or more, than the stoichiometric required quantity.

The necessary amount of citric acid and ammonia in the mixtures is presented rationally in this paper.

ACKNOWLEDGMENTS

This work was partially supported by the strategic grant POSDRU/159/1.5/S/137070 (2014) of the Ministry of Labor, Family and Social Protection, Romania, co-financed by the European Social Fund – Investing in People, within the Sectoral Operational Programme Human Resources Development 2007-2013.

REFERENCES

1. Pullar R.C., *Prog. Mater. Sci.*, 57(7), **2012**, 1191-1334.
2. Guolong T. and Xiuna C., *J. Magn. Magn. Mat.*, 327, **2013**, 87-90.
3. Gutfleisch O., Willard M.A., Brück E., Chen C.H., Sankar S.G. and Ping Liu J., *Advan. Mat.*, 23(7), **2011**, 821–842.
4. Harris V.G., Chen Z.H., Chen Y.J., Yoon S., Sakai T., Gieler A., Yang A., He Y.X., Ziemer K.S., Sun N.X. and Vittoria C., *J.Appl.Phys.*, 99, **2006**, 08M911.
5. Capraro S., Chatelon J.P., Le Berre M., Joisten H., Rouiller T., Bayard B., Barbier D. and Rousseau J.J., *Journal of Magnetism and Magnetic Materials*, 272, **2004**, 1805–E1806.
6. Primac D., Makovec D., Lisjak D. and Drofenik M., *Nanotechnology*, 20(31), **2009**, 315605.
7. Ozgur U., Alivov Y.I. and Morkoc H., *J. Mater. Sci.: Mater. Electron.*, 20(9), 2009, 789-834.
8. Ozgur U., Alivov Y.I. and Morkoc H., *J. Materials Science: Mater. Electron*, 20(10), **2009**, 911-952.
9. Li J., Zhang H.W., Li Y.X., Liu Y.L. and Ma Y.B., *Chin. Phys. B*, 21(1), **2012**, 017501.
10. Yu H.F., *J. Magn. Magn. Mat.*, 341, 2013, 79-85.
11. Mosleh Z., Kameli P., Ranjbar M. and Salamati H., *Ceram. Intern.*, 40(5), **2014**, 7279-7284.
12. Abendini Khorrami S., Islampour R., Bakhtiari H. and Sadr Manuchehri Naeini Q., *International Journal of Nano Dimension*, 3(3), **2013**, 191-197.
13. Meng Y.Y., He M.H., Zeng Q., Jiao D.L., Shukla S., Ramanujan R.V. and Liu Z.W., *J. Alloys Compounds*, 583, **2014**, 220-225.
14. Mohsen Q., *J. Alloys Compd*, 500, **2010**, 125-128.
15. Yamauchi T., Tsukahara Y., Sakata T., Mori H., Chikata T., Katoh S. and Wada Y., *J. Magn. Magn. Mater.*, 321(1), **2009**, 8-11.
16. Virk H.S., Sharma P. and Jotania R., *International Journal of Advanced Engineering Technology*, II(I), **2011**, 131-143.
17. Mihoc G., Ianos R. and Pacurariu C., *Water. Sci. Technol.*, 69(2), **2014**, 385-391.
18. Ianos R., Pacurariu C. and Mihoc G., Ceramics *International*, 40(8B), **2014**, 13649-13657.
19. Li Y., Wang Q. and Yang H., *Current Applied Physics*, 9, **2009**, 1375-1380.
20. Qiu J., Le L. and Gu M., *Materials Science and Engineering A.*, 393, **2005**, 361-365.
21. Mali A. and Ataie A., *Ceramics International*, 30, **2004**, 1979–1983.
22. Lazau I., Ianos R., Pacurariu C., Sinteza si procesarea micro si nanomaterialelor, Editura Politehnica, Timisoara, **2011**.

Received: 06 November 2014
Accepted: 10 December 2014